ISAT v2.0: An integrated tool for nested domain configurations and model-ready emission inventories for WRF-AQM

Kun Wang[1,6], Chao Gao[2], Kai Wu[3], Kaiyun Liu[4, *], Haofan Wang[5], Mo Dan[1], Xiaohui Ji[1, *], Qingqing Tong[2]

[1] Institute of urban safety and environmental science, Beijing academy of science and technology, Beijing 100054, China
[2] Key Laboratory of Wetland Ecology and Environment, Northeast Institute of Geography and Agroecology, Chinese Academy of Sciences, Changchun, 130102, China
[3] Department of Land, Air, and Water Resources, University of California, Davis, CA, USA
[4] State Key Joint Laboratory of Environment Simulation and Pollution Control, School of Environment, Tsinghua University, Beijing 100084, China6
[5] School of Atmospheric Sciences, Sun Yat-sen University, Zhuhai, Guangdong, China
[6] Key Laboratory of Marine Environmental Science and Ecology, Ministry of Education, Ocean University of China, Qingdao, 266100, China

Correspondence: Kaiyun Liu (liuky2021@tsinghua.edu.cn); Xiaohui Ji (jixiaohui@bmilp.com)

Abstract. The ISAT (Inventory Spatial Allocation Tool) v2.0 is an integrated tool that has been developed to configure nested domains, downscale regional emission inventories, allocate local emission inventories, and generate model-ready emission inventories for the Weather Research and Forecasting (WRF)-Air Quality numerical model (AQM). The tool consists of four modules, namely "Prepgrid", "Downscale", "Mapinv", and "Prepmodel", which is designed to perform specific tasks. The "Prepgrid" module utilizes a nested domain configuration algorithm based on WRF-AQM nested rules and the target domain shapefile; "Downscale" module establishes a "sub-grid nearest" method to downscale the regional emission inventory based on spatial surrogate, thereby improving the accuracy and computational efficiency of the process. "Mapinv" module allocates a user-defined regional/city-level emission inventory to grid level based on the target domain shapefile and the spatial surrogate; Finally, "Prepmodel" module generates the model-ready inventories by introducing unique user-friendly emission sector IDs using abbreviations and speciation profiles based on species in the emission inventory and chemical mechanisms, which is available for both the CMAQ and CAMx model. The ISAT v2.0 tool provides a user-friendly solution for model users to configure and run WRF-AQM. And it provides a framework and related algorithms for researchers to develop similar tools for WRF-AQM.

1 Introduction

High spatial-temporal resolution emission inventories (HREIs) of air pollutants are essential for atmospheric environmental mitigation strategies, ambient air quality forecasting, and research on air pollution, as they can quantify pollutant concentrations based on an air quality model (AQM), such as the Weather Research and Forecast (WRF)-Community Multiscale Air Quality (CMAQ) model (Burnett et al., 2018; H. Wang et al., 2022; K. Wang et al., 2022). Preparing HREIs

requires spatial allocation, temporal allocation, and chemical speciation. Spatial allocation maps areas and point emissions into the AQM domain based on source locations and spatial surrogates (Z. Huang et al., 2021; Zheng et al., 2021; Zhou et al., 2017). Temporal allocation provides hourly emissions based on temporal profiles, such as monthly production statistics, heating degree days and temporal variation in traffic activity (K. Wang et al., 2021a). Chemical speciation produces speciated emissions for specific mechanism, such as CB05 or SAPRC99, based on speciation profiles that provide the composition of organic gases and particulate matter in sectors (Huang et al., 2015).

The downscaling of regional emission inventory (REI) disaggregated atmospheric emissions from a national or regional scale to the grid level, providing a method for obtaining an HREI for an AQM, such as the MEIC, with a spatial resolution of 0.25° (ECJRC, 2017; Li et al., 2017; Zheng et al., 2018). The process involves using a spatial surrogate to represent a fraction of the total national/regional emission on a target grid between zero and one (Eyth and Hanisak, 2003). Proxies such as population density, land use, and road maps were developed as spatial surrogates for the intensity of real activity in residential, agriculture, transportation, and other sectors (Lin et al., 2022; Wang et al., 2017). Nearest method is a popular downscaling method, which locates the closet REI value on the target grid and allocates emissions using spatial surrogates (Zhang et al., 2014; Zhuang et al., 2022). However, the use of this method may amplify the emission mismatch without considering a projection difference that may exist between the AQM and the REI, which may be caused by the changes of research domain. The intersect method splits the target domain into several parts between the target domain and the REI, which accounts for the projection difference but may lead to low calculation efficiency. Therefore, a new algorithm is necessary to improve both calculation efficiency and accuracy in the REI downscaling process.

Various emission inventory processing tools have been developed previously, yet an integrated tool for domain configuration to model-ready inventory workflow for WRF-AQMs in unavailable. For example, TEMMS can only support the emission of transportation (Namdeo et al., 2002), and THOSCANE cannot create a model-ready emission inventory for AQM (Monforti and Pederzoli, 2005). SMOKE, a Linux-platform supported and widely used tool in AQM, requires a predefined spatial surrogate from other geoprocessing tools, such as ArcGIS, and cannot define parameters for nested domains in WRF-AQM (Baek and Seppanen, 2021). The WRF Domain Wizard (https://esrl.noaa.gov/gsd/wrfportal/DomainWizard.html) allows the user to configure nested domains by manually delimiting research areas. However, without the shapefile of the target area, obtaining precise domains is challenging, which requires several trials and expert experience to obtain suitable nested domains in AQMs. Therefore, it is essential to develop an integrated tool that ensures domain consistency and provides a user-friendly workflow, from a nested domain configuration to the WRF-AQM system.

Innovatively, a user-friendly and integrated tool, ISAT (Inventory Spatial Allocation Tool) v2.0, was developed from nested domain configuration to model-ready emission inventory for WRF-AQM in this study. We established a nested domain configuration algorithm based on shapefile that ensure domain consistency between the WRF, AQM and emission inventory. We proposed a regional inventory downscaling algorithm called the "sub-grid nearest method," which improved the computational efficiency and accuracy of the REI downscaling. We provided interfaces for a model-ready emission

inventory for CMAQ and CAMx models. In addition, we embedded population- and road-based spatial surrogate data into the ISAT, which supports most spatial allocation workflows for WRF-AQM in China.

2 Materials and methods

We developed an integrated tool to complete the workflow from nested domain configuration to model-ready HREI for WRF-AQM, as depicted in Figure 1. The shapefiles provide location and extent in each domain and used to configure nested domains in WRF-AQM by "Prepgrid" module. For domains without local emission inventory, REIs, such as the MEIC, can be downscaled into domains by "Downscale" module. Local emission inventories can be allocated into domains by "Mapinv" module. Both of CMAQ and CAMx model support inline plume rise calculations and inline format HREI (Guevara et al., 2014). Based on gridded emissions from "Downscale" and "Mapinv", the inline format HREI for WRF-AQM can be created in "Prepmodel". Users can adopt each module individually or in combination according to their needs. The methodological innovations in this study included a nested domain configuration algorithm, a sub-grid nearest method, a user-friendly emission source ID and speciation profiles, as detailed in the following sections.

2.1 Nested domain configuration in "Prepgrid"

Using Arakawa-C grid staggering in WRF model, 3:1 grid-distance nesting ratio between domains is required for nested domain configuration (Skamarock et al., 2019). Nested domains can be classified into parent and child domains and initially configured based on the extent of shapefiles (Daniels et al., 2016). The outermost domain determines the projection in WRF-AQM. The child domains need to be extended based on user needs and 3:1 grid-distance nesting ratio between domains. Users can set the number of extended grids in the east, west, south, and north directions as needed: (add_e, add_w, add_s and add_n). The number of grids that must be expanded under grid-distance nesting rules were also considered: (add_x and add_y). Taking the x-direction as an example, add_e, add_w and add_x were used to extent the domain in the WRF model, as shown in Figure 2. Moreover, due to the outermost cells in WRF are inappropriate to use in AQM(USEPA,2019), "*model_clip*" was conduct to define lateral boundary for AQM, as shown in **Appendix. A**. In practice, we usually obtain the extent of the study area based on its shapefile. Compared with manual configuration, using shapefile can provide consistent and accurate nested domain between WRF, AQM and emission inventory. The major steps and key parameters are described below.

2.1.1 Projection configuration based on the outmost domain

Standard parallels, central meridian, and latitude of the lambert conformal conic (LCC) projection can be obtained from the shapefile in the outmost domain. Due to defined grid spacing, the WRF-AQM domain may exceed the study area's shapefile; thus, the shapefile center does not represent the center of the LCC projection. We designed four main steps to accomplish projection configuration: i) Setting standard parallels. Standard parallels were defined by users according to the location of

the outmost domain (for example, Shanxi province configured with 33° and 42°). ii) Setting extent and number of grids in domain. Under the LCC projection in the previous step and the shapefile, we obtained the number of grids (num_x and num_y) and origin (X_{min} and Y_{min}) as shown in Eqs. (1–4). iii) Updating LCC projection. Transferred center of the domain into WGS 84 projection and used to update the center in LCC projection. iv) Getting final LCC projection parameters. Looped through steps "iii) –ii) – iii)" until the difference in the center in domain and shapefile in the loops could be ignored.

$$num_x = Roundup\left(\frac{disx}{dx}\right) + add_e + add_w , \tag{1}$$

$$num_y = Roundup\left(\frac{disy}{dy}\right) + add_s + add_n, \tag{2}$$

$$X_{min} = \frac{-(num_x \times dx)}{2}, \tag{3}$$

$$Y_{min} = \frac{-(num_y \times dy)}{2}, \tag{4}$$

where, $disx$ and $disy$ is the length of the shapefile in the x- and y-directions.

2.1.2 Determination of child domain parameters

Constrained by grid-distance nesting rules and lateral boundaries for the AQM, the child domain configuration step is different from the parent domain step. Spatial resolution and origin in the parent and child domains (dx_{par}, dx_{child}, $xstart_{child}$, and $xstart_{parent}$) were adopted for the child domain configuration. Taking the x-direction as an example, the number of grids was calculated based on the spatial coverage of the shapefile, user-defined parameters, and the number of grids constrained by the nesting rules in the WRF model, as shown in Eq. (5). add_x is the must-add number of grids according to the nesting rules and the shapefile in the parent and child domain, as shown in Eq. (6), and num_x was further corrected by Eq. (7-8). X_{min} is the present start position of the child domain with a projection configuration based on the nesting rules and the user-defined add_w as shown in Eq. (9). Moreover, $start_x$ denotes the starting position for the child domain in the parent domain, which can be used to configure nested domain in the WRF model in Eq. (10).

$$num_{x,tmp} = Roundup\left(\frac{disx_{child}}{dx_{child}}\right) + add_e + add_w + add_x, \tag{5}$$

$$add_x = Roundup\left(\frac{xstart_{child} - int\left(\frac{xstart_{child} - xstart_{parent}}{dx_{par}}\right) \times dx_{par} - xstart_{parent}}{dx_{child}}\right), \tag{6}$$

$$tmpgrid_x = mod\left(num_{x,tmp}, \frac{dx_{par}}{dx_{child}}\right), \tag{7}$$

$$num_x = \begin{cases} num_{x,tmp} \ (tmpgrid_x = 0) \\ num_{x,tmp} + \frac{dx_{par}}{dx_{child}} - tmpgrid_x \ (tmpgrid_x \neq 0) \end{cases}, \tag{8}$$

$$120 \quad X_{min} = integer\left(\frac{xstart_{child} - xstart_{parent}}{dx_{par}}\right) \times dx_{par} + xstart_{parent} - dx_{child} * add_w, \tag{9}$$

$$start_x = \frac{X_{min} - xstart_{parent}}{dx_{par}}, \tag{10}$$

2.2 Sub-grid nearest method in "Downscale"

Intersect and nearest methods are commonly used to downscale REI into user-defined domains. The intersect method obtains overlapping areas between the REI and the target domain, while the nearest method assigns emissions based on the nearest
125 REI value. The intersect method accurately reflects the spatial relationship between the target domain and the REI. However, if there are evident projection and spatial resolution differences between REI and the target domain, a large number of small intersections are created, which significantly decreases calculation efficiency. The nearest method addresses this limitation, but may lead to emission mismatches due to spatial differences. For example, the nearest method ignored the orange grid emissions but exaggerated the contribution of the yellow grids in the research domain, as shown in Figure 3. To fully
130 consider the advantages and disadvantages of these two algorithms, we used the "sub-grid nearest" method to allocate the emission inventory, as shown in Eqs. (11–13). Figure 3 depicts the process we used to obtain the REI values using the nearest and sub-grid nearest methods. The colors in the figure represent the REI values, and the symbols (such as *) represent the grid ID. First, we introduced a "sub-grid ratio" to divide each grid into p sub-grids, such as nine sub-grids in each grid. Second, we adopted the conventional nearest method to locate the nearest REI values for each sub-grid. Third, we
135 calculated the emissions for each sub-grid based on the nearest REI value and spatial surrogates. Finally, we obtained the emissions for each grid based on a summary of the sub-grid emissions in each grid. It should be ensured that $SA_{region,I_{i,j,p}}$ is larger or equal to the sum of $SA_{target,i,j,p}$ in the same region grid $I_{i,j,p}$ based on the principle of mass conservation. This module can downscale regional emission inventories user-friendly and easy-to-use based on default or user-defined proxy without external tools such as ArcGIS.

$$140 \quad E_{target,i,j} = \sum_p E_{target,i,j,p}, \tag{11}$$

$$E_{targe,i,j,p} = E_{region,I_{i,jp}} \times R_{region,I_{i,jp}} \times \frac{SA_{target,i,j,p}}{SA_{region,I_{i,j,p}}}, \tag{12}$$

$$I_{i,j,p} = Nearest\left(Grid_{targe,i,j,p}, Grid_{region}\right), \tag{13}$$

where, i,j are the column and row number of the target grid; p is the sub-grid ID in grid (i,j); $E_{target,i,j}$ is the emissions in grid (i,j); $E_{target,i,j,p}$ is the emissions in sub-grid p in grid (i,j); $I_{i,j,p}$ is the location of sub-grid p for the target grid (i,j) in the
145 region domain; $E_{region,I_{i,jp}}$ are the regional emissions in $I_{i,j,p}$; $SA_{region,I_{i,j,p}}$ is the spatial allocator for region grid $I_{i,j,p}$; $SA_{target,i,j,p}$ is the spatial allocator for sub-grid p of target grid (i,j); $Grid_{region}$ is the domain of the REI; and $Grid_{targe,i,j,p}$ is the sub-grid p of target grid (i,j).

2.3 User-friendly emission source sector ID in "Prepmodel"

User-friendly emission source sector IDs (EIDs) are source abbreviations, for example, AG for agriculture. EID is a unique ID for the emission source sector in ISAT and defined new sources friendly. Speciate and temporal profiles for sectors can be easily defined with EID, as shown in **Table 1**, where the speciate profile and point emission inventory are prefixed by "Speciate_" and "STACK_GROUP_" and suffixed by an EID, respectively. The area emission inventory was named EID. To define a temporal profile for each sector, users can add columns labeled by EID in hourly.csv, weekly.csv, and monthly.csv, as shown in **Table 2**. Users can easily add or delete sources in model-ready emission inventory by their needs in "Prepmodel"

2.4 User-friendly speciation profile structure in "Prepmodel"

Compared with multiple input file types for chemical speciation in the SMOKE model, including GSCNV, GSPRO, GSPRODESC, GSPRO_COMBO, GSREF, and GSTAG files, this tool simplifies the process with individual speciate profiles for each sector. An example of a speciate profile is shown in **Table 3**. Here, "pollutant" denotes the pollutants in the emission inventory; "species" denotes the pollutants in the chemical mechanism adopted in the AQM; "split_factor" represents the fraction of the "pollutant" emission to "species" in the AQM between zero and one, and it must be mass conservative; "unit" is the unit of species adopted in the AQM, as "moles/s" for gaseous pollutants and "g/s" for particulate pollutants; and "divisor" converts mass-based speciation into mole-based speciation, with molar mass for gaseous pollutants and a default value (set to 1) for particulate pollutants. Therefore, the user can easily modify the speciation profile based on the chemical mechanism in the AQM and the pollutants in the emission inventory.

In addition, we embedded a gridded spatial surrogate for roads and populations in the ISAT. The road database was obtained from the OpenStreetMap, with four levels, including motorway, secondary, primary, and residential road. The standard road length (Zheng et al., 2009), based on vehicle speed, number of lanes, and road width from the Code for Transport Planning on Urban Roads (GB 50220-95) in China, was used to calculate the gridded road map data. Population density data based on the 2020 LandScan Global Population Database (Rose et al., 2021) can used in ISAT with NetCDF format. Users can also prepare any proxy for their needs. For example, land use and POIs data are recommended for agriculture and residential sectors (Wang et al., 2017; Huang et al., 2022). Due to the nearly 1km resolution of the ISAT-embedded gridded population and road maps, users can generate HREIs with finer spatial resolution ≥1km.

3 Case studies

As the capital of China, Beijing has a large number of population and vehicles, making it a hotspot for air pollution research in China (Gao et al., 2018; X. Huang et al., 2021). This study presents three nested domain cases: mainland China, Beijing-Tianjin-Hebei (BTH), and Beijing (BJ), with spatial resolutions of 27, 9, and 3 km, respectively, as shown in Figure 4. The ISAT was used for the workflow from the nested domain configuration to the model-ready inventory for the WRF-AQM.

The shapefile for these domains was used to configure nested domains in the WRF-AQM and to create the ready emission inventory in the "Prepgrid" module. Provincial census of pollutant sources in transportation and residential sectors in Beijing (BMEEP, 2020) were allocated into 3km×3km grids by the "Mapinv" module. The MEIC regional emission inventory with spatial resolution of 0.25°×0.25° in 2020 was downscaled to grid level in the "Downscale" module.

3.1 Nested domain configuration by "Prepgrid"

ISAT provides comprehensive grid information for the WRF-AQM in comma-separated values (csv) file and shapefile formats. Csv format data contains grid information for each domain and can be further used as the input for other ISAT modules. Shapefile formatted data can be displayed directly in ArcGIS or other geographic information system to display and check the configuration for nested domains. "Domainname" and "Casename" were used to mark the output in the "Prepgrid" module. "${Casename}_gridinfo.csv" summarizes grid information in nested domains and can be used to configure domain parameters in the WRF model, as shown in Figure 5(b). "wrf_${Domainname}.shp" and "wrf_${Domainname}.csv" provided shapefile and grid information for the ISAT-configured WRF model. "aqm_${Domainname}.shp" and "aqm_${Domainname}.csv" were the shapefile and grid information for the ISAT-configured AQM model. Due to blend of larger-scale driving data and scale-specific physics, the outermost cells in WRF domain are inappropriate to use and usually removed in AQM (USEPA,2019). The ISAT-configured domains reflect this requirement of lateral boundary in AQM and accurately obtain the WRF-AQM domain.

3.2 Downscaled regional emissions inventory by "Downscale"

The MEIC inventory is widely used in China. In this study, the 2020 annual MEIC emissions were preprocessed into csv format and downscaled into the AQM domain by "Downscale" module. Compared with ArcGIS, SMOKE and other tools, using "Dowanscale" module reduces the timeliness from hours to minutes. We compared gridded residential emissions in BTH under different downscaled method, including intersect method, nearest and sub-grid nearest methods. The sub-grid ratio, the key parameter in the sub-grid nearest method, must be either one or a multiple of three and applied to test the allocation result. Therein, the nearest method can be configured with a sub-grid ratio equal to one. With the sub-grid ratio increased from one to nine, the spatial allocation was close to the result of the intersect method for the urban area, as shown in Figure 6. The sub-grid method with a sub-grid ratio equal to three significantly improved the allocation compared to the nearest method, and the R squared increased from 0.91 to 0.98. The increase in the sub-grid ratio from three to nine slightly improved the distribution results, with R squared increasing from 0.979 to 0.984, as shown in Figure 7. Although a higher sub-grid ratio may lead to a more accurate allocation, one needs to consider the computational efficiency and resolution of the spatial surrogate. For example, the running time of "downscaled" module increased from 2 minutes to 10 minutes with the sub-grid ratio increased from 3 to 9 in this case. In addition, for REI grids with empty spatial surrogates, ISAT applies the grid area as a weight when allocating emissions. Constrained by the spatial surrogate (≤1) for each REI grid based on principle of mass conservation, the downscaled emission inventory exhibited good agreement with the REI. Regarding the

result of intersect method as the true value, the relative error of total $PM_{2.5}$ emissions under each sub-grid ratio is less than 0.2 %, which reflects the good quality of the downscaling in terms of mass flux conservation.

These downscaled REI can be used to produce model-ready emission for domains without local emission inventory. Due to more detailed and realistic emission characteristics, local emission inventory is highly recommended on spatial-temporal emission characteristic research and simulation in WRF-AQM in the innermost domain.

3.3 Gridded local emission inventory by "Mapinv"

Differing from the downscale process used for the gridded REI described in Section 3.2, mapping the provincial/city-level local emission inventory onto the grid level required the identification of region attributes for each AQM domain and the allocation of emissions based on spatial surrogates. In ISAT v2.0, user can add a column to define the region in the shapefile and input the local emission inventory in the "localinv" file. ISAT will allocate the local emission inventory for each species to grid level. Taking Beijing as an example, emissions for the occupied residential (RE) and transportation sectors were 7,763 t NOx, 25,900 t VOCs, and 22,700 t NOx, 2,654 t VOCs, respectively. The gridded emission inventory for the RE and TR sectors created by the ISAT reflected the spatial variations in population density and the road map in Beijing, as shown in Figure 8. Based on the embedded population density and road map, ISAT could flexibly allocate the local emission inventory to grid level.

3.4 Model-ready emission inventory by "Prepmodel"

User can generate inline format model-ready emission inventories for AQM using "Prepmodel" module. The gridded emission inventory, generated by "Mapinv" and "Downscale," can be used as area emission input files. The point emission file was organized into csv format which contained emission, locations, and stack parameters with reference to the SMOKE model. Temporal profile files were defined based on statistical data and previous studies. The speciation profiles for sectors were obtained from the SPECIATE database or field measurements. Moreover, GRIDCRO2D files generated by the Meteorology-Chemistry Interface Processor in the CMAQ model was applied to provide global attributes and configurations consistent with the AQM. "Runtime" was used to define the model-ready emission timesteps for the AQM. The ISAT inline format emission inventory was named EID. For example, "TR.nc" denoted the area emission source for the TR sector. "PPpoint.nc" and "STACK_GROUP_PP.nc" represented hourly emission and the source information for the power plants, respectively. The model-ready emission inventory can be directly used in AQMs, such as CMAQ and CAMx, as well as instrumental modules, such as DDM and ISAM. Previous studies achieved reliable simulations result using this approach (H. Wang et al., 2021; K. Wang et al., 2022, 2021a, 2021b; Liu et al., 2023; Li, 2021; Tan, 2022).

The configurations and steps used in these cases are detailed in the Appendix. A.

4 Conclusion

240

We have developed an integrated tool, ISAT v2.0 that streamlines the workflow from nested domain configuration to model-ready emission inventory for WRF-AQM. ISAT v2.0 consists of four main modules: Prepgrid, Downscale, Mapinv, and Prepmodel. The "Prepgrid" module can accurately provide user-defined domain configuration under nesting rules in WRF-AQM and the shapefile of the study area. It can also configure the namelist.wps file in WPS, using domain parameters

245 defined in this module. The "Downscale" module conducted with the "sub-grid nearest" method significantly improved the allocation result with the nearest method. Moreover, users can flexibly set the "sub-grid ratio" according to their specific needs. The "Mapinv" module provides a user-friendly tool to allocate provincial/city-level local emission inventory to grid level using user-defined shapefiles and local emission inventories. Finally, the "Prepmodel" module can generate an inline format model-ready file emission inventory for WRF-AQM and provides users the numerical simulations. ISAT is free,

250 expansible, and supported by both Linux and Windows, and can be applied to process other regional emission inventories, such as REAS, by providing grid templates and updating user-defined spatial surrogates. Relying on the established relationship between the shapefile and the WRF-AQM domain, ISAT is highly extendable, including the creation of ocean files in CMAQ models (USEPA,2019), the labeling of source regions in CAMX-PSAT, and other potential uses.

Code and data availability. The current version of ISAT is available from the project website: https://github.com/ISAT-Office/ISAT under the GNU General Public License v3. The source code of ISAT v2.0 and input data used to produce the results used in this paper is archived on Zenodo at https://doi.org/10.5281/zenodo.7481439 (Wang *et al.,* 2022).

255

Author contribution. Kun Wang: Conceptualization, Methodology, Software, Writing-Original draft. Chao Gao, Kai Wu and Haofan Wang: Data Curation; Mo Dan: Writing-Reviewing and Editing; Kaiyun Liu and Xiaohui Ji: Resources. Supervision, Investigation.

260

Competing interests. No competing interests are present.

Acknowledgements. This work was supported by the National Key Research and Development Program of China (2019YFE0194500), Natural Science Foundation of China Youth Project (42207248), BJAST Scientific Research in 2022(11000022T000000468154), BJAST Scientific Research in 2022(11000022T000000468176), and the European Union's Horizon 2020   Research and Innovation programmes under grant agreement no 870301 (AQ-WATCH).

265

Appendix A. ISAT step-by-step guide

Taking nested domains in "Mainland China-BTH-BJ" with spatial resolution of "27km-9km-3km" as example.

Step 1: Obtain nested domain parameters for WRF-AQM based on domain shapefile.

(a) Give the information of "par.ini" in "Prepgrid" model.

lat1:33.0	# First standard latitude for LCC	
lat2:42.0	# Second standard latitude for LCC	
casename:3nestdomain	# Case name	
numdom:3	# Number of nested domains	
shpath: ./shp/mainlandchina.shp, ./shp/JJJ.shp,./shp/beijing.shp	# Shpfile path for domains	
dx:27000,9000,3000	# Resolution in meters for domains	
xladd:2,3,3	#Added grid in left in x direction	
xradd:2,3,3	#Added grid in right in x direction	
ytadd:2,3,3	#Added grid in top in y direction	
ydadd:2,3,3	#Added grid in down in y direction	
domainname:MainlandChina,JJJ,Beijing	#Name for domains	
model_clip:1,1,1	#Clip number of grids for AQM	

(b) Running prepgrid module by "python prepgrid.py". Domain information summarized in "3nestdomain_gridinfo.csv",
270 detailed below.

domid	centlon	centlat	xmin	ymin	numx	numy	xstart	ystart
0	102.0737	36.68731	-2484000	-2119500	184	157	0	0
1	102.0737	36.68731	945000	-40500	66	93	127	77
2	102.0737	36.68731	1116000	382500	63	72	19	47

Therein, you can define WPS domain using variables above:

parent_id	1	1	2
parent_grid_ratio	1	3	3
i_parent_start	1	$xstart(1)+1	$xstart(2)+1
j_parent_start	1	$ystart(1)+1	$ystart(2)+1
e_we	$numx(0)+1	$numx(1)+1	$numx(2)+1
e_sn	$numy(0)+1	$numy(1)+1	$numy(2)+1
ref_lat	$centlat		
ref_lon	$centlon		
truelat1	$lat1		
stand_lon	$centlon		
truelat2	$lat2		

(c) You can get fishnet shapefile for WRF model named "wrf_"+${domainname}+ ".shp" and AQM model named "aqm_"
+$domainname+ ".shp".

(d) You can also get gridded information for domains in "wrf_" +${domainname}+ ".csv" for WRF model and "aqm_" +$domainname+ ".shp" for AQM model respectively.

Step 2: Downscaling regional emission inventory into target domains.

(a) Give the information of "par.ini" in "Downscale" module.

invf:./input/domain/aqmJJJ.csv	# Path of target domain information
dx:9000	# Resolution in meters for target domain
ratio:3	# Subgrid ratio
emissions: ./regioninv/agricultureannual.csv,./regioninv/transportationannual.csv,./regioninv/residentialannual.csv	# Path for regional emission inventory
casename:JJJ	# Case name
method:area,road,pop	# Allocation method for specific emission inventory area: based on grid area road: based on roads map pop: based on population map

(b) Running downscale module by "python downscale.py". And getting gridded emission for specific area sources.

Step 3: Preparation of model-ready emission inventories for AQM.

(a) Give the information of "par.ini" in "prepmodel" module.

runtime:193	# Time steps for AQM run
gridcro2d: ./src/met/GRIDCRO2D_9km	#MCIP generated GRIDCRO2D file
speciate: ./src/speciate/speciate_AR.csv, ./src/speciate/speciate_AG.csv	# Speciation profile for area emission sources.
speciate_groups: ./src/speciate/speciate_IN.csv	# Speciation profile for point emission sources.
temporary_hour : ./src/temporary/hourly.csv	# Hourly temporal profile for emission sources.
temporary_week : ./src/temporary/weekly.csv	# Weekly temporal profile for emission sources.
temporary_month: ./src/temporary/monthly.csv	# Monthly temporal profile for emission sources.
emissions: ./src/emissions/MEIC/AR.csv, ./src/emissions/MEIC/AG.csv	#Path of area emission files
stack_groups: ./src/emissions/MEIC/STACK_GROUP_IN.csv	#Path of point emission files

(b) Run prepmodel module by "python area_emis.py; python point_emis.py; python point_info.py". For CAMx model, CMAQ2CAMx can be used transfer this output into CAMx.

Other step: Mapping local emission inventory into grid level.

(a) Give the information of "par.ini" in "mapinv" model.

regionshp:./input/Region/BJ.shp	# Shapefile for region
Key:NAME	#Region column in shapefile
grid:./input/Grid/3km.csv	# Grid information by "pregrid'
sapath:./input/SA/inv_sa_tmp_road.csv,./input/SA/inv_sa_tmp_pop.csv	# Spatil surrogated by "downscale" module
localinv:./input/localinv/TR.csv,./input/localinv/RE.csv	# Path way for local emission inventory
localname:TR3KM,AR3KM	# Name of gridded emission inventory output

285 (b) Run mapinv module by "python mapinv.py"

References

Baek, B.H., Seppanen, C., 2021. CEMPD/SMOKE: SMOKE v4.8.1 Public Release (January 29, 2021). https://doi.org/10.5281/ZENODO.4480334

Burnett, R., Chen, H., Szyszkowicz, M., et al. 2018. Global estimates of mortality associated with long-term exposure to
290   outdoor fine particulate matter. Proc. Natl. Acad. Sci. U.S.A. 115, 9592–9597. https://doi.org/10.1073/pnas.1803222115

Daniels, M. H., Lundquist, K. A., Mirocha, J. D., et al. 2016. A New Vertical Grid Nesting Capability in the Weather Research and Forecasting (WRF) Model, Monthly Weather Review, 144(10), 3725-3747.

European Commission. Joint Research Centre (ECJRC)., 2017. Downscaling methodology to produce a high-resolution gridded emission inventory to support local/city level air quality policies. Publications Office, LU.

295 Eyth, A.M., Hanisak, K., 2003. The MIMS Spatial Allocator: A Tool for Generating Emission Surrogates without a Geographic Information System.

Gao, J., Wang, K., Wang, Y., et al. 2018. Temporal-spatial characteristics and source apportionment of PM2.5 as well as its associated chemical species in the Beijing-Tianjin-Hebei region of China. Environmental Pollution 233, 714–724. https://doi.org/10.1016/j.envpol.2017.10.123

300 Guevara M, Soret A, Arévalo G, et al. 2014. Implementation of plume rise and its impacts on emissions and air quality modelling [J]. Atmos. Environ., 99: 618-29.

Huang, C., Zhuang, Q., Meng, X. et al. 2022. A fine spatial resolution modelling of urban carbon emissions: a case study of Shanghai, China. Sci Rep 12, 9255. https://doi.org/10.1038/s41598-022-13487-5

Huang, C., Wang, H.L., Li, L., et al. 2015. VOC species and emission inventory from vehicles and their SOA formation
305   potentials estimation in Shanghai, China. Atmos. Chem. Phys. 15, 11081–11096. https://doi.org/10.5194/acp-15-11081-2015

Huang, X., Tang, G., Zhang, Junke, et al, 2021. Characteristics of PM2.5 pollution in Beijing after the improvement of air quality. Journal of Environmental Sciences 100, 1–10. https://doi.org/10.1016/j.jes.2020.06.004

Huang, Z., Zhong, Z., Sha, Q., et al. 2021. An updated model-ready emission inventory for Guangdong Province by incorporating big data and mapping onto multiple chemical mechanisms. Science of The Total Environment 769, 144535. https://doi.org/10.1016/j.scitotenv.2020.144535

Li, M., Liu, H., Geng, G., et al. 2017. Anthropogenic emission inventories in China: a review. National Science Review 4, 834–866. https://doi.org/10.1093/nsr/nwx150

Li, Y. 2021. Study on Ozone Formation Sensitivity in the Pearl River Delta based on Satellite Remote Sensing and Air qualify Model. Master's Thesis, South China University of Technology.

Lin, P., Gao, J., Xu, Y., et al. 2022. Enhanced commercial cooking inventories from the city scale through normalized emission factor dataset and big data. Environmental Pollution 120320. https://doi.org/10.1016/j.envpol.2022.120320

Liu S., Liu, K., Wang, K., et al. 2023. Fossil-Fuel and Food Systems Equally Dominate Anthropogenic Methane Emissions in China. Environmental Science & Technology. 2023, 57, 6, 2495–2505. https://doi.org/10.1021/acs.est.2c07933

Monforti, F., Pederzoli, A., 2005. THOSCANE: a tool to detail CORINAIR emission inventories. Environmental Modelling & Software 20, 505–508. https://doi.org/10.1016/j.envsoft.2004.07.001

Namdeo, A., Mitchell, G., Dixon, R., 2002. TEMMS: an integrated package for modelling and mapping urban traffic emissions and air quality. Environmental Modelling & Software 17, 177–188. https://doi.org/10.1016/S1364-8152(01)00063-9

Rose, A., McKee, J., Sims, K., et al. 2021. LandScan Global 2020. https://doi.org/10.48690/1523378

Skamarock, W.C., Klemp, J.B., Dudhia, J., et al. 2019. A Description of the Advanced Research WRF Model Version 4. UCAR/NCAR. https://doi.org/10.5065/1DFH-6P97

Tan, X. 2022.Construction of CMAQ Pollution Source Inventory Based on ISAT Model. Master's Thesis, Jilin University.

USEPA. 2019.CMAQ User's Guide.https://github.com/USEPA/CMAQ/blob/main/DOCS/Users_Guide/

Wang, H., Liu, Z., Wu, K., et al. 2022. Impact of Urbanization on Meteorology and Air Quality in Chengdu, a Basin City of Southwestern China. Front. Ecol. Evol. 10, 845801. https://doi.org/10.3389/fevo.2022.845801

Wang, H., Liu, Z., Zhang, Y., et al. 2021. Impact of different urban canopy models on air quality simulation in Chengdu, southwestern China. Atmospheric Environment 267, 118775. https://doi.org/10.1016/j.atmosenv.2021.118775

Wang, K., Gao, J., Liu, K., et al. 2022. Unit-based emissions and environmental impacts of industrial condensable particulate matter in China in 2020. Chemosphere 303, 134759. https://doi.org/10.1016/j.chemosphere.2022.134759

Wang, K., Gao, J., Tian, H., et al. 2017. An emission inventory spatial allocate method based on POI data. China Environmental Science 37, 2377–2382.

Wang, K., Tong, Y., Yue, T., et al. 2021a. Measure-specific environmental benefits of air pollution control for coal-fired industrial boilers in China from 2015 to 2017. Environmental Pollution 273, 116470. https://doi.org/10.1016/j.envpol.2021.116470

Wang, K., Tong, Y., Gao, J., et al. 2021b. Pinpointing optimized air quality model performance over the Beijing-Tianjin-Hebei region: Mosaic approach. Atmospheric Pollution Research 12, 101207. https://doi.org/10.1016/j.apr.2021.101207

Wang, K., Gao C., Wang, H., et al. 2022. Inventory Spatial Allocate Tool v2.0 source code, Zenodo, https://doi.org/10.5281/zenodo.7481439.

345   Zhang, X., Gurney, K. R., Rayner, P., et al. 2014. Sensitivity of simulated CO_2 concentration to regridding of global fossil fuel CO_2 emissions. Geosci. Model Dev., 7, 2867–2874, https://doi.org/10.5194/gmd-7-2867-2014.

Zheng, B., Cheng, J., Geng, G., et al. 2021. Mapping anthropogenic emissions in China at 1 km spatial resolution and its application in air quality modeling. Science Bulletin. 66, 612–620. https://doi.org/10.1016/j.scib.2020.12.008

Zheng, B., Tong, D., Li, M., et al. 2018. Trends in China's anthropogenic emissions since 2010 as the consequence of clean
350   air actions. Atmos. Chem. Phys. 18, 14095–14111. https://doi.org/10.5194/acp-18-14095-2018

Zheng, J., Che, W., Wang, X., et al. 2009. Road-Network-Based Spatial Allocation of On-Road Mobile Source Emissions in the Pearl River Delta Region, China, and Comparisons with Population-Based Approach. Journal of the Air & Waste Management Association 59, 1405–1416. https://doi.org/10.3155/1047-3289.59.12.1405

Zhou, Y., Zhao, Y., Mao, P., et al. 2017. Development of a high-resolution emission inventory and its evaluation and
355   application through air quality modeling for Jiangsu Province, China. Atmos. Chem. Phys. 17, 211–233. https://doi.org/10.5194/acp-17-211-2017

Zhuang, J., Dussin, R., Huard, D., et al. 2022. xESMF: v0.7.0 (v0.7.0). Zenodo. https://doi.org/10.5281/zenodo.7447707
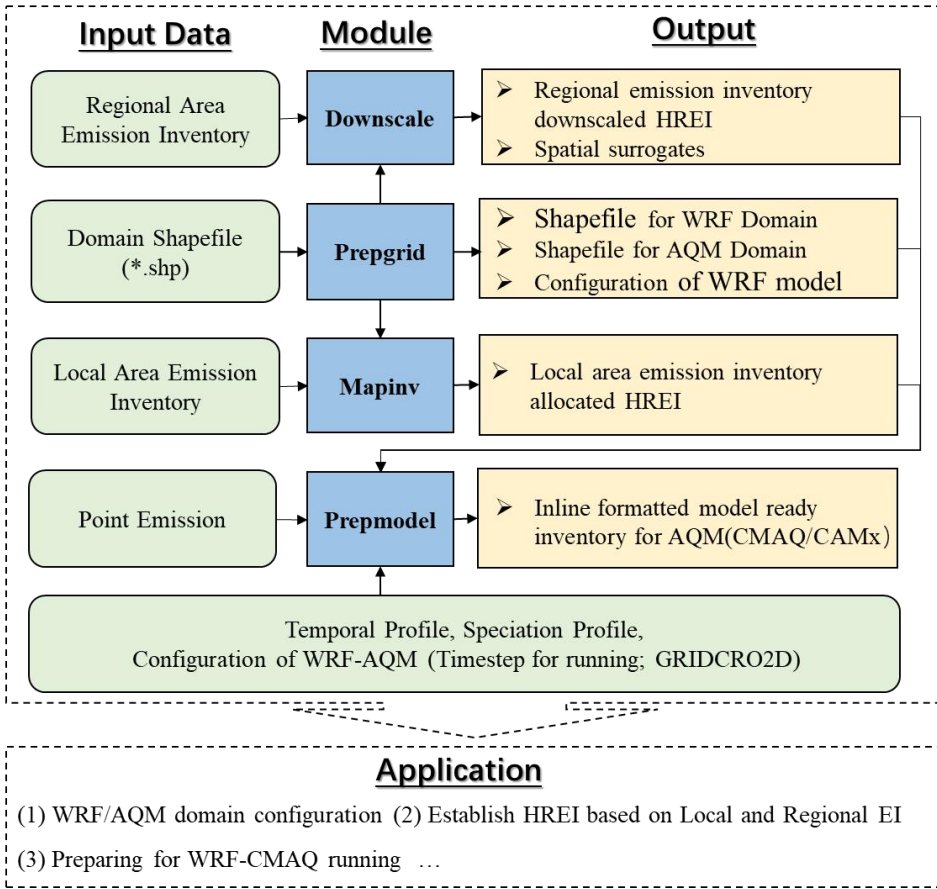
Figure 1. ISAT framework.
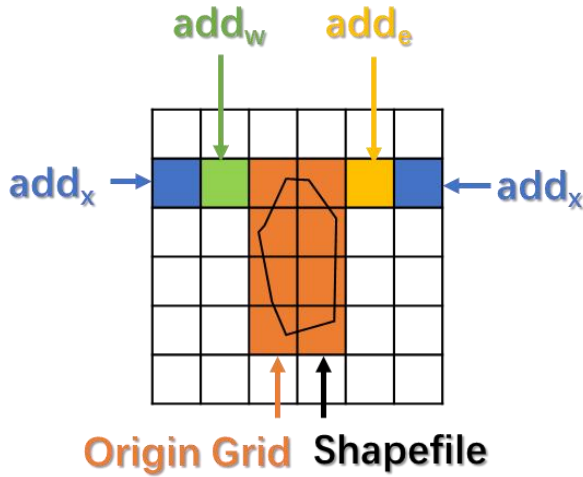
360

Figure 2. Parameters for modifying the domain in the x-direction.

"+", "-", "*" and "o" denote grid ID in target domain
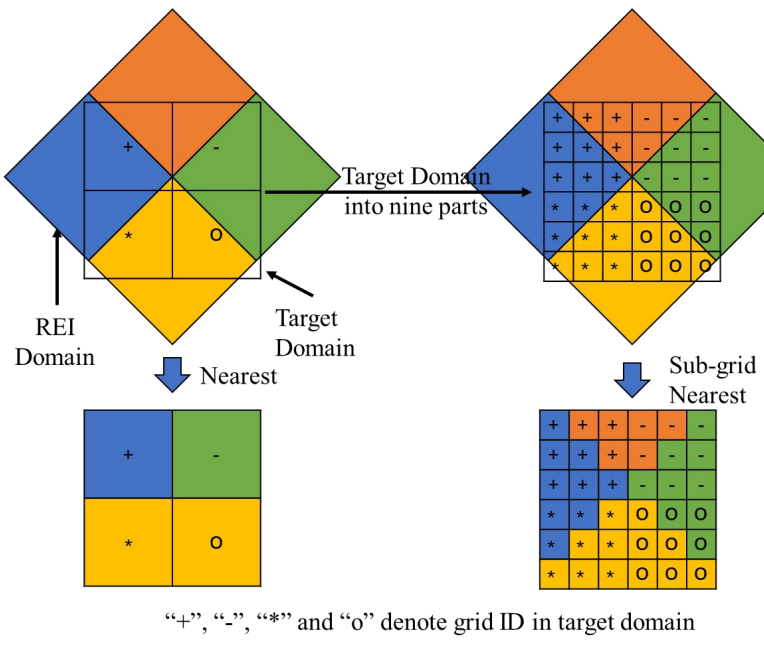
Figure 3. Concept of the sub-grid nearest method.
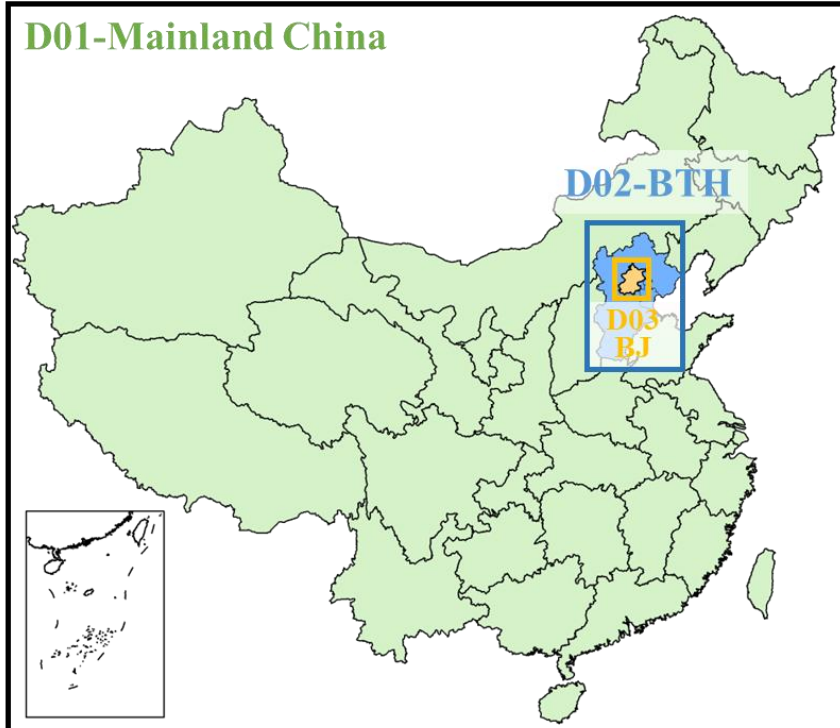
365   **Figure 4. The three nested domains and their shapefiles.**
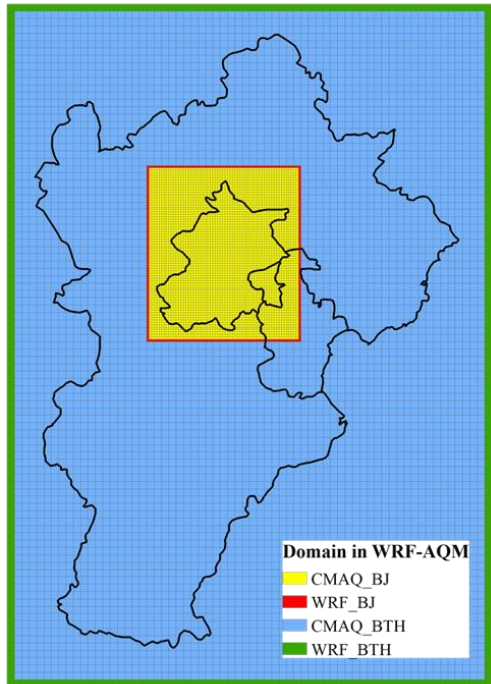
(a)
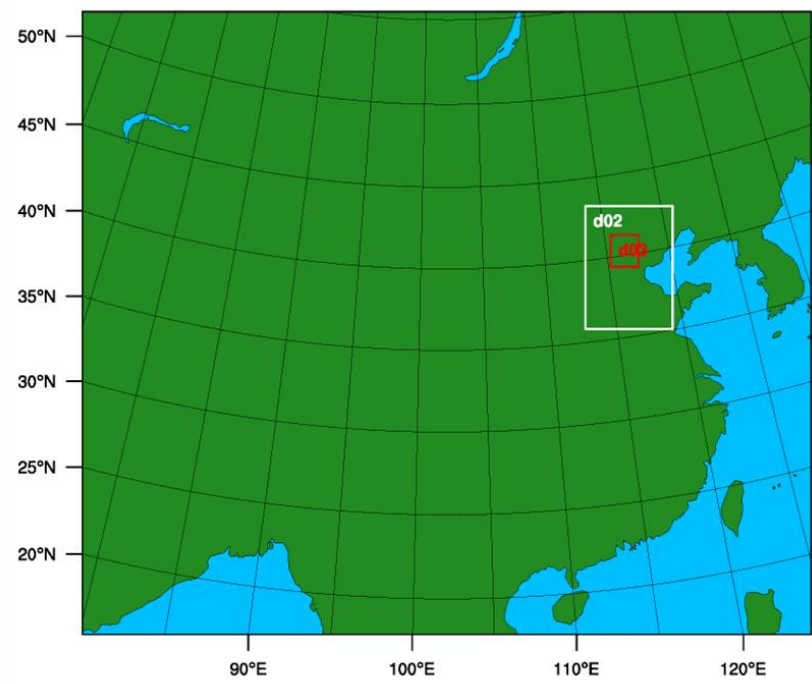
(b)

Figure 5. ISAT-configured WRF-AQM nested domains.
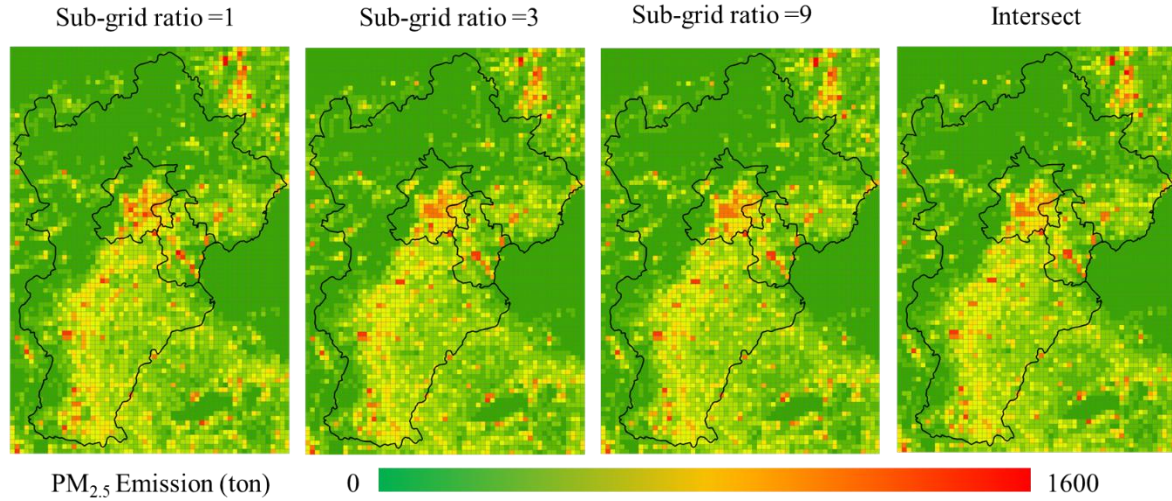
Figure 6. Comparison of the intersect and the sub-grid nearest method allocations with different sub-grid ratios.

370
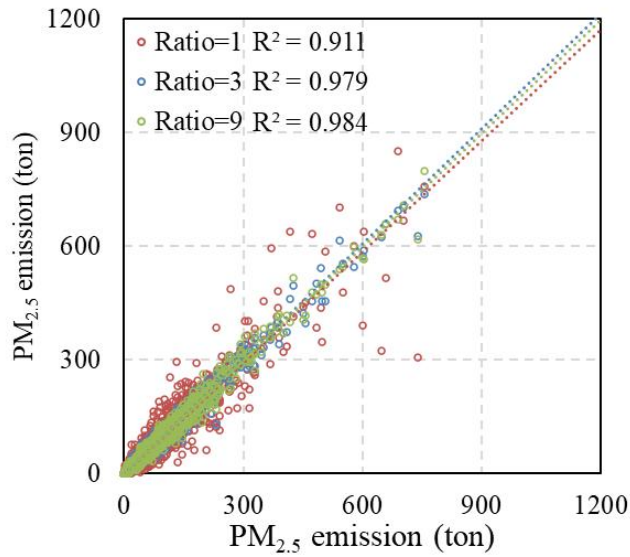
Figure 7. Pairwise relationship between the intersect and sub-grid nearest methods with different sub-grid ratios for particulate matter (PM).

375
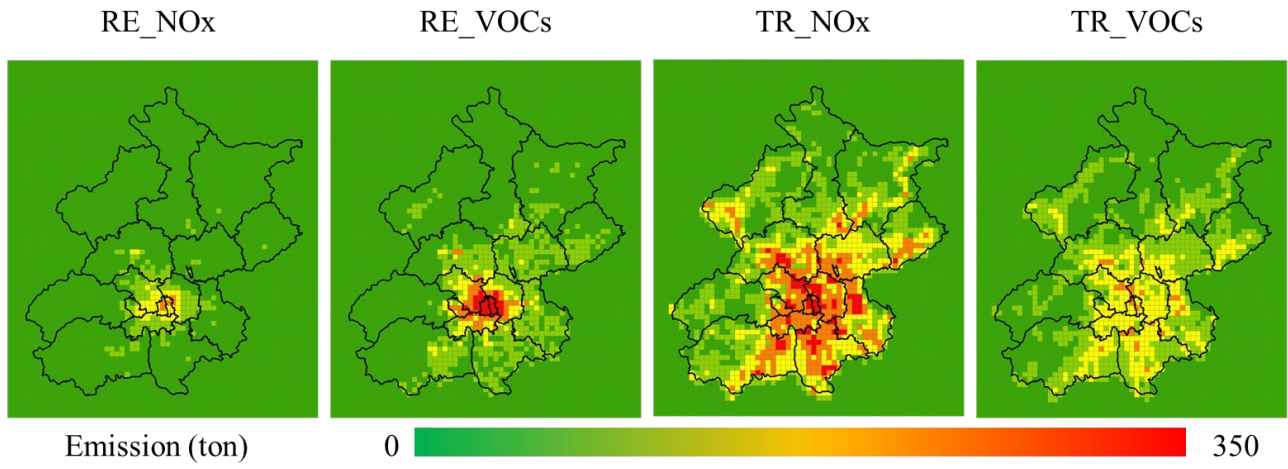
Figure 8. Spatial allocation for Beijing.

Table 1. File structure defined by emission source sector ID (EID)

File Type	Filename	Example
Speciate profile	Speicate_$EID.csv	Speciate_IN.csv; Speciate_PP.csv; Speciate_AG.csv; Speciate_AR.csv
Area Emission	$EID.csv	AR.csv; AG.csv
Point Emission	STACK_GROUP_$EID.csv	STACK_GROUP_IN.csv; STACK_GROUP_PP.csv

Table 2. Case of temporal profiles (for PP source)

hourly.csv		weekly.csv		monthly.csv	
hourly*	PP	weekly	PP	monthly	PP
0	0.045	0	0.145	1	0.090
1	0.047	1	0.144	2	0.065
2	0.046	2	0.143	3	0.083
3	0.045	3	0.144	4	0.075
4	0.043	4	0.143	5	0.075
…	…	5	0.138	…	…
23	0.044	6	0.143	12	0.098

*: UTC time

Table 3. Case of speciate profile in ISAT

pollutant	species	split_factor	divisor	unit	pollutant	species	split_factor	divisor	unit
CB05_ALD2	ALD2	1.00	44	mole/s	PM2.5	PH2O	0.00	1	g/s
CB05_ALDX	ALDX	1.00	45	mole/s	PM2.5	PK	0.00	1	g/s
CB05_ETH	ETH	1.00	28	mole/s	PM2.5	PMG	0.00	1	g/s
CB05_ETHA	ETHA	1.00	30	mole/s	PM2.5	PMN	0.00	1	g/s
CB05_ETOH	ETOH	1.00	46	mole/s	PM2.5	PMOTHR	0.06	1	g/s
CB05_FORM	FORM	1.00	30	mole/s	PM2.5	PNA	0.00	1	g/s
CB05_IOLE	IOLE	1.00	55	mole/s	PM2.5	PNCOM	0.10	1	g/s
CB05_ISOP	ISOP	1.00	68	mole/s	PM2.5	PNH4	0.01	1	g/s
CB05_MEOH	MEOH	1.00	32	mole/s	PM2.5	PNO3	0.00	1	g/s
CB05_NVOL	NVOL	1.00	1	mole/s	PM2.5	POC	0.63	1	g/s
CB05_OLE	OLE	1.00	30	mole/s	PM2.5	PSI	0.00	1	g/s
CB05_PAR	PAR	1.00	17	mole/s	PM2.5	PSO4	0.01	1	g/s
CB05_TERP	TERP	1.00	136	mole/s	PM2.5	PTI	0.00	1	g/s
CB05_TOL	TOL	1.00	101	mole/s	SO2	SO2	1.00	64	mole/s
CB05_UNR	UNR	1.00	19	mole/s	SO2	SULF	0.01	98	mole/s
CB05_XYL	XYL	1.00	114	mole/s	NH3	NH3	1.00	17	mole/s
PM2.5	PAL	0.00	1	g/s	CO	CO	1.00	28	mole/s
PM2.5	PCA	0.00	1	g/s	PMcoarse	PMC	1.00	1	g/s
PM2.5	PCL	0.00	1	g/s	NOx	NO	0.90	30	mole/s
PM2.5	PEC	0.18	1	g/s	NOx	NO2	0.09	46	mole/s
PM2.5	PFE	0.00	1	g/s					